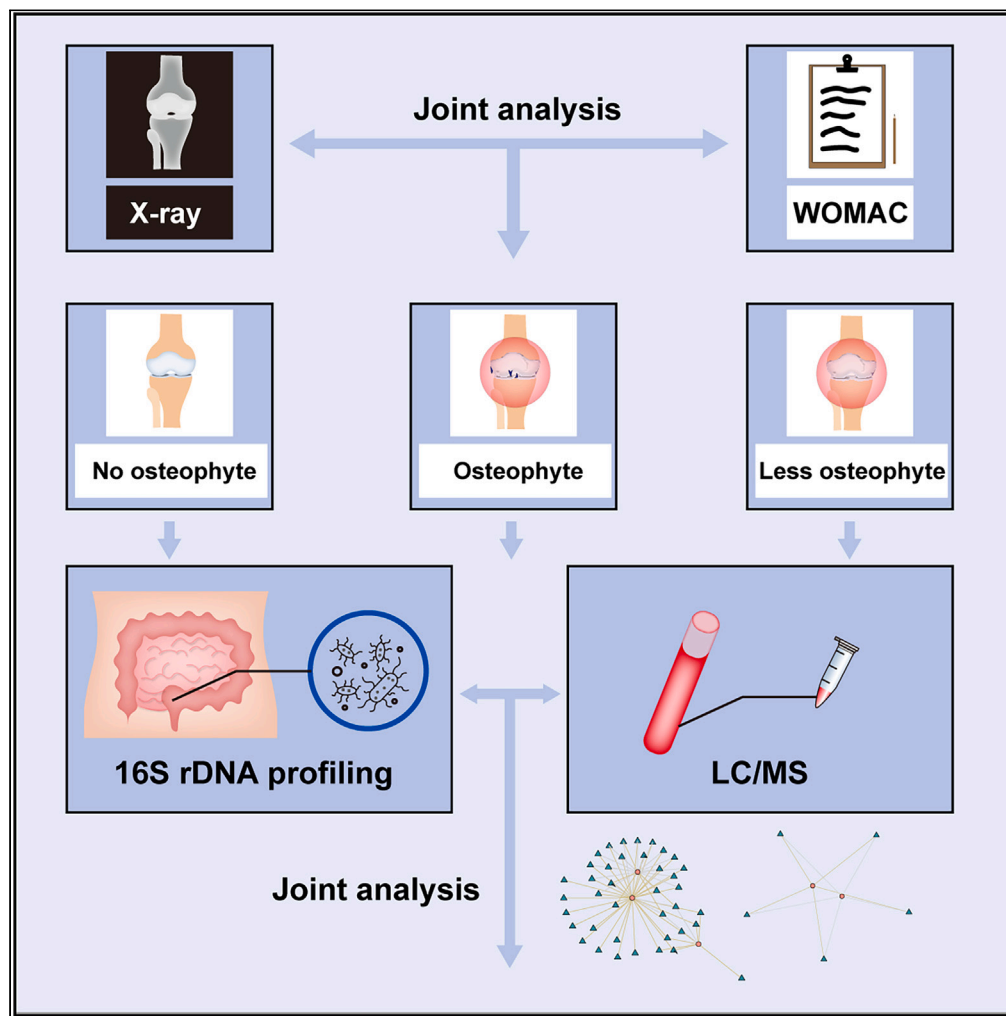## Article

Diet influences knee osteoarthritis osteophyte formation via gut microbiota and serum metabolites

Dandan Zhu,
Xiaochao Wang,
Zhihui Xi, ...,
Xiaolong Zeng,
Huolun Feng, Da
Guo

xiaolzeng@126.com (X.Z.)
fenghuolun2022@qq.com (H.F.)
david.guo.d@gzucm.edu.cn
(D.G.)

Highlights

Higher Blautia levels in gut
microbiota may contribute
to osteophyte formation in
KOA

LTB4 and PGD2 may serve
as biomarkers linked to
osteophyte formation in
KOA

Five metabolites , fecal
Blautia levels negatively
correlated with cheese
consumption

Article

Diet influences knee osteoarthritis osteophyte formation via gut microbiota and serum metabolites

Dandan Zhu,[1,9] Xiaochao Wang,[2,9] Zhihui Xi,[3,4,9] Kunling Chen,[5,9] Yatian Feng,[6] Chunjian Zi,[2] Zhijian Pan,[2] Xinyu Ma,[2] Xiaolong Zeng,[7,*] Huolun Feng,[3,4,10,*] and Da Guo[8,*]

SUMMARY

Osteophyte formation, a key indicator of osteoarthritis (OA) severity, remains poorly understood in its relation to gut microbiota and metabolites in knee osteoarthritis (KOA). We conducted 16S rDNA sequencing and untargeted metabolomics on fecal and serum samples from 20 healthy volunteers, 80 KOA patients in Guangdong, and 100 in Inner Mongolia, respectively. Through bioinformatics analysis, we identified 3 genera and 5 serum metabolites associated with KOA osteophyte formation. Blautia abundance negatively correlated with meat, cheese, and bean consumption. The 5 serum metabolites negatively correlated with dairy, beef, cheese, sugar, and salt intake, yet positively with age and oil consumption. Higher Blautia levels in the gut may contribute to KOA osteophyte formation, with serum metabolites LTB4 and PGD2 potentially serving as biomarkers. KOA patients in Inner Mongolia exhibited lower Blautia levels and reduced expression of 5 serum metabolites, possibly due to cheese consumption habits, resulting in less osteophyte formation.

INTRODUCTION

Osteoarthritis (OA) continues to be a widespread cause of disability,[1] affecting approximately 13.8% of the population,[2] with a significant prevalence observed among women and rural residents.[3] The escalating incidence of OA can be attributed not only to prolonged life expectancy but also to factors including obesity and chronic inflammation stemming from sedentary lifestyles and unhealthy dietary habits.[4] Unfavorable lifestyle choices play a central role in precipitating OA,[5] sparking growing interest in investigating the relationship between gut microbiota and OA.

Recent studies indicate that the gut microbiota may play a substantial role in the pathogenesis and increased susceptibility to OA by participating in interactions that encompass mechanical, cellular, and biochemical factors.[6] Disruptions in the composition of gut microbiota are suggested to serve as a connecting link between adverse factors and the development of OA.[7] The impact of gut microbiota and metabolites on the progression of OA is evidenced by their ability to regulate the intestinal mucosal barrier, intestinal metabolites, and immune responses.[8]

Osteophyte, defined as the ectopic bone formation within a joint,[9,10] holds significant importance in the pathogenesis of OA,[11] serves as a marker of OA severity,[12] and is incorporated into OA diagnostic criteria.[13] The initiation and advancement of osteophyte formation in KOA have been linked to factors such as estrogen levels, femoral neck T-scores, and hypertension.[14] However, despite these associations, no studies have explored the correlation between osteophyte formation and gut microbiota and metabolites in KOA.

An initial observation suggested that KOA patients in Inner Mongolia typically displayed fewer osteophytes on X-ray imaging compared to those in Guangdong, where a higher prevalence of osteophytes was noted (Figures 1A–1C). To further investigate this phenomenon, we undertook a comprehensive study involving 16S rDNA sequencing on fecal samples collected from both healthy volunteers and KOA patients in Guangdong and Inner Mongolia. Additionally, we conducted liquid chromatography-tandem mass spectrometry (LC-MS/MS)-based untargeted metabolomics analysis on serum samples.

[1]Guangdong Center for Clinical Laboratory, Guangdong Provincial People's Hospital (Guangdong Academy of Medical Sciences), Southern Medical University, Guangzhou, Guangdong 510080, China
[2]The Second Clinical Medical College of Guangzhou University of Chinese Medicine, Guangzhou, Guangdong 510405, China
[3]School of Medicine, South China University of Technology, Guangzhou, Guangdong 510006, China
[4]Department of Gastrointestinal Surgery, Department of General Surgery, Guangdong Provincial People's Hospital (Guangdong Academy of Medical Sciences), Southern Medical University, Guangzhou, Guangdong 510080, China
[5]Southern Medical University, Guangzhou, Guangdong 510515, China
[6]Rehabilitation department, The Second People's Hospital of Baiyun District, Guangzhou, Guangdong 510450, China
[7]Department of Orthopaedic Surgery, The Second Affiliated Hospital of Guangzhou University of Chinese Medicine, Guangzhou, Guangdong 510120, China
[8]Department of Orthopaedic Surgery, Guangdong Provincial Hospital of Chinese Medicine, Guangzhou, Guangdong 510120, China
[9]These authors contributed equally
[10]Lead contact
*Correspondence: xiaolzeng@126.com (X.Z.), fenghuolun2022@qq.com (H.F.), david.guo.d@gzucm.edu.cn (D.G.)
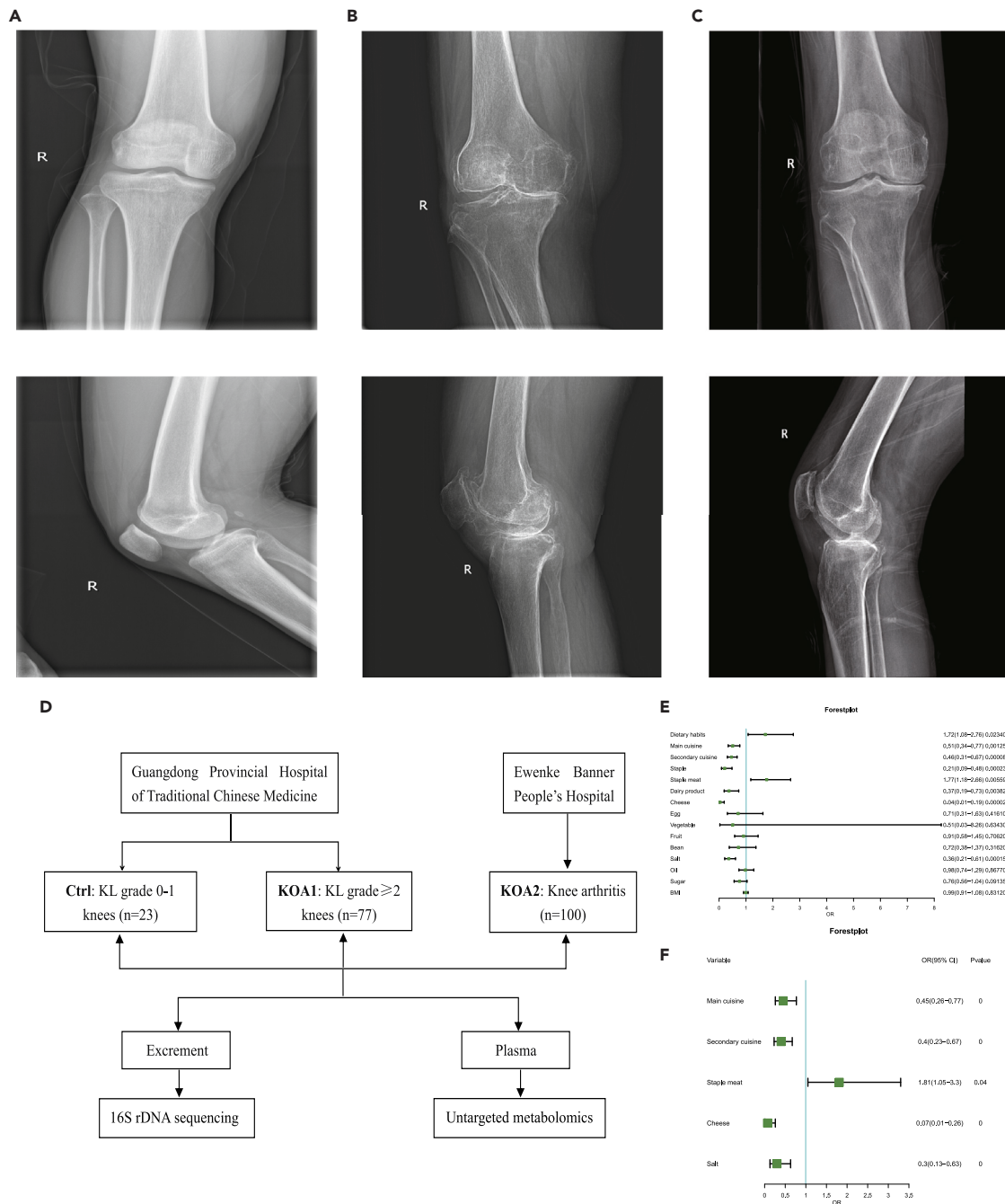https://doi.org/10.1016/j.isci.2024.110111

Figure 1. Representative knee X-ray imaging and clinical characteristics of study participants

Orthopantomograms and lateral images of the right knee joints of (A) healthy volunteers, (B) patients with KOA from Guangdong Provincial Hospital of Chinese Medicine and (C) patients with KOA from Ewenke Banner People's Hospital.

(D) Flow chart of the study. We recruited healthy volunteers and patients with knee osteoarthritis in Guangdong Provincial Hospital of Chinese Medicine and Ewenke Banner People's Hospital. Informed consent was obtained from the participants in all cases. Fecal samples and serum samples were collected from the participants, and 16S rDNA sequencing and Untargeted metabolomics were used, respectively.

(E) Univariate and (F) multivariate logistic regression analyses were performed to analyze the presence or absence of osteophyte with clinical characteristics. See also STAR Methods and Table S1.
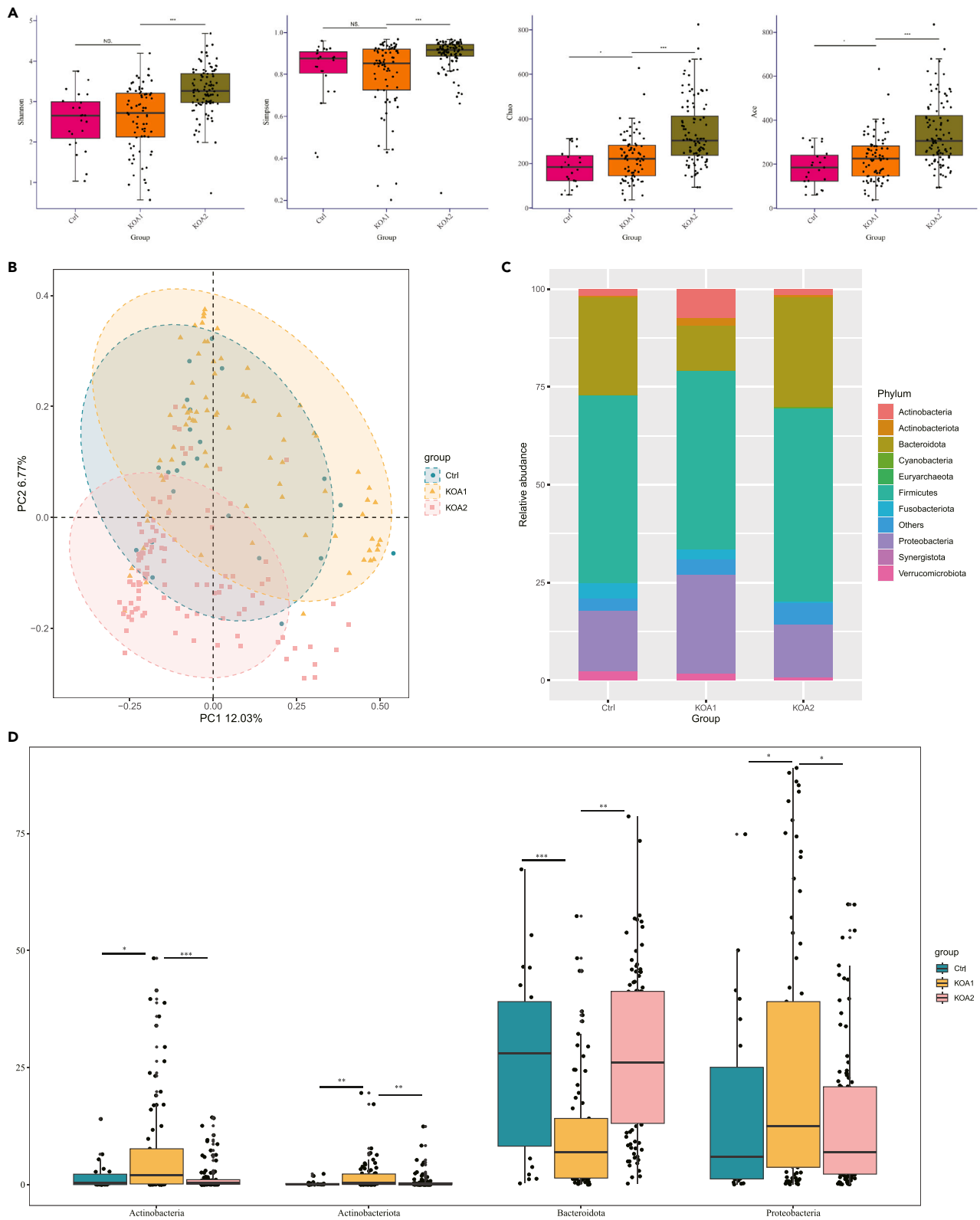
Figure 2. Comparative analysis of species diversity and relative abundance at the phylum level associated with osteophyte formation in KOA

(A) Alpha diversity by Shannon, Simpson, Chao, and Ace indices.

(B) Beta diversity was measured using principal coordinate analysis (PCoA).

(C) The distribution plot of relative abundance at the phylum level.

(D) The Wilcoxon test showed that 4 phyla were significantly altered in the KOA1 group compared to the Ctrl and KOA2 groups. NS, not significant. *p*-value, *$p < 0.05$; **$p < 0.01$; ***$p < 0.001$. See also STAR Methods and Figure S1B.

The investigation sought to elucidate variances and interplays in gut microbiota and metabolites among KOA patients classified under Kellgren-Lawrence (K-L) grades 0–1 (referred to as the Ctrl group, denoting the absence of osteophytes) and those categorized under K-L grades 2–4 (referred to as the KOA1 group, indicating the presence of osteophytes) in Guangdong. This examination was further corroborated with KOA patients in Inner Mongolia (referred to as the KOA2 group, representing individuals with fewer osteophytes). The objective was to evaluate gut microbiota composition in fecal samples from KOA patients, along with the abundance of serum metabolites, and their correlation with osteophyte occurrence. This study holds potential for offering valuable insights into refining dietary recommendations tailored specifically to KOA patients.

RESULTS

Clinical characteristics of study participants

The study encompassed 20 healthy volunteers and 80 KOA patients from Guangdong Provincial Hospital of Chinese Medicine in the Guangdong region, along with 100 KOA patients from Ewenke Banner People's Hospital in the Inner Mongolia region. Participants in the Guangdong region with K-L classification grades 0–1 constituted the Ctrl group (no osteophyte group), while those with K-L classification grades 2–4 were categorized as the KOA1 group (osteophyte group). Patients with KOA in the Inner Mongolia region were designated as the KOA2 group (less osteophyte group). There were no significant differences among the Ctrl, KOA1, and KOA2 groups regarding age, gender, and BMI. However, variations in dietary habits and WOMAC scores were observed. Table S1 provides detailed demographic and clinical characteristics of the study participants. The study process is delineated in Figure 1D.

To further validate the impact of dietary habits on osteophyte formation in KOA, logistic regression analysis was employed. Univariate (Figure 1E) and multivariate (Figure 1F) logistic regression analyses revealed that main cooking methods, secondary cooking methods, staple meat, cheese, and salt were identified as independent risk factors affecting osteophyte formation.

Diversity of gut microbiota

In microbial amplicon 16S sequencing, after quality control and filtering processes, a total of 24,351,522 high-quality 16S rDNA reads were obtained, with a median read number of 12,579,790.5 (range: 4,490,080–14,335,660) per sample (Table S2). Following denoising, a total of 20,813 Amplicon Sequence Variants (ASVs) were identified. The species dilution curves for all samples (Figure S1A) supported the sufficiency of sequencing depth.

Subsequently, the alpha diversity and beta diversity of the gut microbiota were assessed between the Ctrl and KOA1 groups, as well as between the KOA1 and KOA2 groups, through sequence comparison. Concerning the comparison between Ctrl and KOA1 groups, Shannon's and Simpson's indices did not show statistical significance, while Chao's and Ace's indices were statistically significant. In the comparison between KOA1 and KOA2 groups, all four indices mentioned above were statistically significant (Figure 2A). To evaluate the overall differences in beta diversity among the gut microbiota samples from each group, a PCoA score plot was generated using the Bray-Curtis distance (Figure 2B). The results indicated discernible differences in the composition of gut microbiota between the Ctrl and KOA1 groups, as well as between the KOA1 and KOA2 groups.

Changes in the composition of the gut microbiota associated with osteophyte formation in KOA

The examination of relative proportions of dominant taxa at the phylum level between the Ctrl and KOA1 groups, and between the KOA1 and KOA2 groups, revealed 11 identified phyla in each group, with Firmicutes being the most dominant. Actinobacteria, Actinobacteriota, and Proteobacteria were enriched in the KOA1 group, whereas Proteobacteria were reduced (Figures 2C and 2D). This suggests that Actinobacteria, Actinobacteriota, and Proteobacteria may be phyla associated with osteophyte formation in KOA. Additionally, the ratio of Firmicutes/Bacteroidetes (F/B) did not differ in the KOA1 group compared to the Ctrl and KOA2 groups (Figure S1B).

Out of 401 genera, 16 genera showed statistically significant differences between the Ctrl and KOA1 groups ($p < 0.05$) (Table S3), while 91 genera differed significantly between the KOA1 and KOA2 groups ($p < 0.05$) (Table S4). By comparing the intersected differentiated genera between Ctrl and KOA1 groups, and KOA1 and KOA2 groups, and then comparing the KOA1 group with Ctrl and KOA2 groups respectively, 3 obtained intersected differentiated genera, namely Blautia, Granulicatella, and Phascolarctobacterium, exhibited consistent trends. Among them, Blautia and Granulicatella were enriched in the KOA1 group, while Phascolarctobacterium was enriched in the Ctrl and KOA2 groups (Figure 3A). Spearman's correlation analysis showed that Blautia was associated with age, dietary habits, cheese consumption, and bean consumption; Phascolarctobacterium was associated with age; and Granulicatella was associated with the main mode of cooking and staple food (Figure 3B; Table S5). Dietary habits were defined as "1" for omnivore, "2" for vegetarian, and "3" for meat eater. Cheese consumption was defined as "1", and non-consumption of cheese as "0". Bean consumption was defined as "1", and non-consumption of beans was defined as "0". The main cooking methods were defined as "1" for steaming, "2" for sautéing, "3" for boiling, and "4" for other cooking methods. For
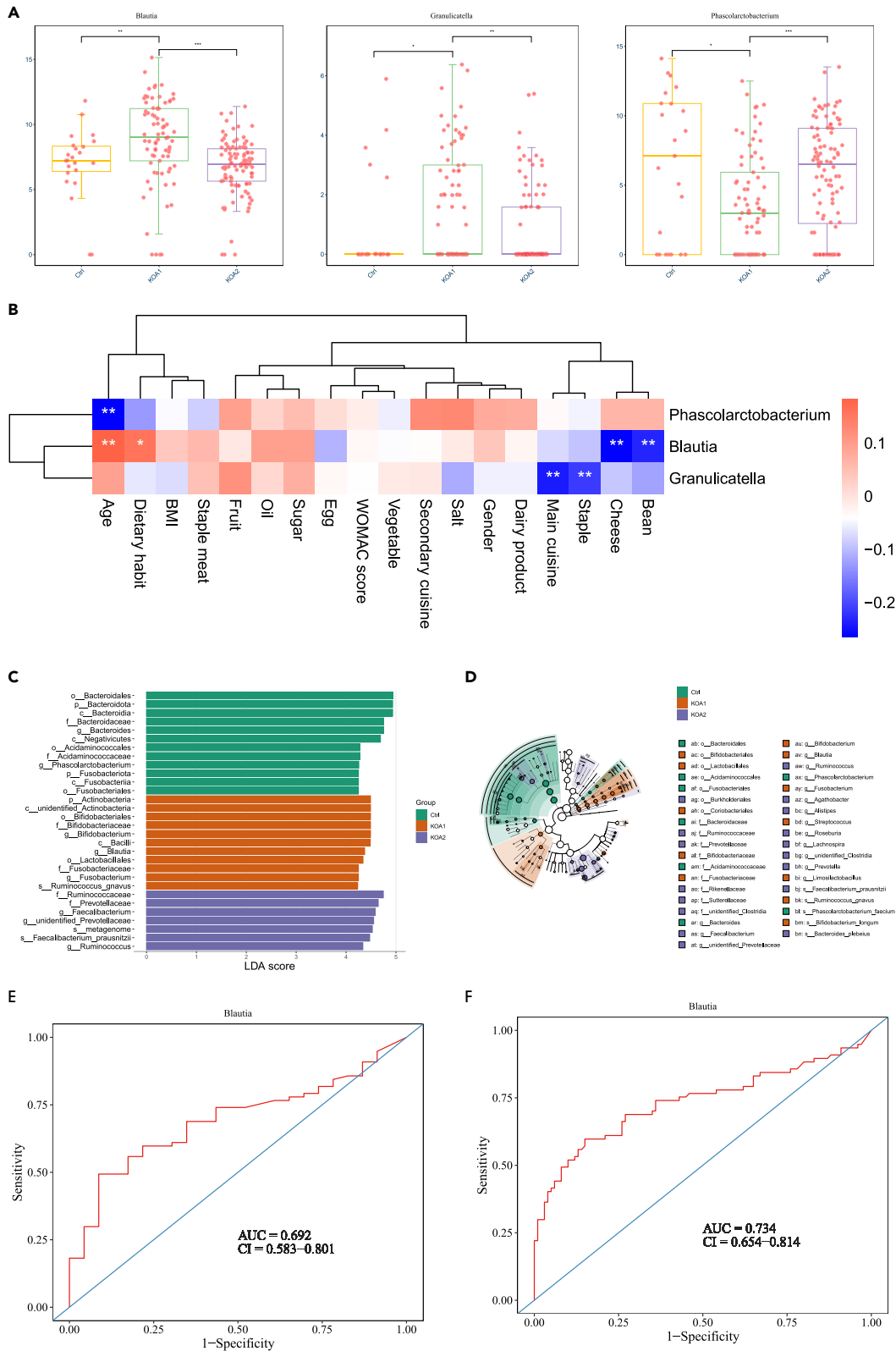
Figure 3. Changes in relative abundance and correlation with clinical characteristics at the genus level associated with osteophyte formation in KOA

(A) The Wilcoxon test showed that 3 genera changed significantly in the KOA1 group compared to the Ctrl and KOA2 groups.

(B) Heatmap of the correlation between the 3 genera and clinical characteristics. Positive correlations are in red; negative correlations are in blue. Regions of significant correlation are indicated by white stars p-value, *p < 0.05; **p < 0.01. Identification of the specific altered taxa using linear discriminant analysis (LDA) and effect size analysis (LEfSe).

(C) Histogram of variance characteristics of the top 30 taxonomic units with the highest LDA (log10).

(D) Phylogenetic trees for specific differential taxa. ROC curves for Blautia in the (E) test cohort and (F) validation cohort. See also Figure S2 and Tables S3, S4, and S5.

staple food, rice was defined as "1", noodles as "2", and other as "3". Consequently, the abundance of Blautia was negatively correlated with meat consumption, cheese consumption, and bean consumption, while the abundance of Granulicatella was negatively correlated with boiled cooking style and noodles.

Next, LEfSe was employed to compare the composition of gut microbiota among the 3 groups to identify specific dominant flora associated with osteophyte formation in KOA. Ultimately, 30 taxa with the highest Linear Discriminant Analysis (LDA) (log10) ($p < 0.01$) were found to be differentially characterized. Among them, Bifidobacterium, Blautia, and Fusobacterium were predominantly enriched in the KOA1 group (Figures 3C and 3D). To investigate the diagnostic accuracy of these 3 genera in distinguishing the KOA1 group from the Ctrl group and the KOA2 group, a receiver operating curve (ROC) analysis was performed. The results showed that Blautia had the largest Area Under the Curve (AUC) value compared to Bifidobacterium and Fusobacterium (Figures S2A and S2B), with AUC values of 0.692 (Figure 3E) and 0.734 (Figure 3F) in the test cohort (Ctrl group vs. KOA1 group) and the validation cohort (KOA1 group vs. KOA2 group), respectively.

Changes in serum metabolic Profiles associated with osteophyte formation in KOA

Given the substantial impact of the gut microbiota on serum metabolites due to complex metabolic pathways,[15] we investigated the characterization of the serum metabolome using an untargeted LC-MS approach. A partial least-squares-discriminant analysis (PLS-DA) model was applied to delineate metabolomic distributions between the Ctrl group and the KOA1 group, as well as between the KOA1 group and the KOA2 group. The results demonstrated metabolic differences between the Ctrl and KOA1 groups, and between the KOA1 and KOA2 groups (Figure 4A). Significance diagnostic plots indicated that the scatter points were below the horizontal line, signifying that the PLS-DA model was not overfitted (Figure 4B). Subsequently, 231 (Table S6; Figures S3A and S3B) and 469 (Table S7; Figures 4C and 4D) differentially enriched metabolites were identified between the Ctrl and KOA1 groups, and between the KOA1 and KOA2 groups, respectively (VIP >1, FC ≥ 1.5, $p < 0.05$). By intersecting the differential metabolites between the Ctrl and KOA1 groups, and between the KOA1 and KOA2 groups, and comparing the KOA1 group with the Ctrl and KOA2 groups respectively, 42 metabolites in the resulting intersection displayed a consistent trend. These serum metabolites were hypothesized to be associated with osteophyte formation in KOA.

Finally, KEGG enrichment analysis of the 42 metabolites revealed that their synthesis was regulated by 6 different metabolic pathways ($p < 0.05$). These pathways included Arachidonic acid metabolism, Serotonergic synapse, Steroid hormone biosynthesis, Inflammatory mediator regulation of TRP channels, Retinol metabolism, and Ovarian steroidogenesis (Figure 4E; Table S8). Notably, Arachidonic acid metabolism and Serotonergic synapse predominantly shared the same 5 metabolites, namely Leukotriene B4, 15(S)-HPETE, prostaglandin D2, Leukotriene A4, and 5(S)-Hydroperoxyeicosatetraenoic acid (Table S9). In comparison with the Ctrl and KOA2 groups, these 5 metabolites were expressed at higher levels in the KOA1 group (Figure 4F). Spearman's correlation analysis was conducted to explore the relationship between the 5 metabolites and clinical characteristics. The results indicated that these metabolites were associated with age, main cooking methods, secondary cuisine, staple meat, dairy product consumption, cheese consumption, salt consumption, and oil consumption (Figure 4G; Table S10). Meat consumption was defined as "1" for beef, "2" for pork, "3" for more than one type of meat, and "4" for other meats. Consequently, the expression levels of the 5 metabolites were negatively correlated with dairy product consumption, beef consumption, cheese consumption, sugar and salt consumption, and positively correlated with age and oil consumption. To evaluate the diagnostic accuracy of these 5 metabolites in distinguishing KOA1 from the Ctrl group and KOA2, a ROC analysis was performed. The results revealed that the AUC of the 5 metabolites, Leukotriene B4, 15(S)-HPETE, prostaglandin D2, Leukotriene A4, and 5(S)-Hydroperoxyeicosatetraenoic acid, was greater than 0.9 in both the test and validation cohorts (Figures 4H and 4I).

Relationship between gut microbiota and serum metabolites associated with osteophyte formation in KOA

To illuminate the intricate interactions between gut microbiota and serum metabolites linked to osteophyte formation in KOA, we conducted Spearman's correlations between the 3 genera and 42 metabolites (Table S11). Subsequently, major interactions were elucidated by constructing co-occurrence network diagrams (r > 0.2, $p < 0.05$, Figure 5A). In Figure 5A, Blautia and Phascolarctobacterium emerged as core genera associated with the majority of metabolites. Blautia exhibited predominantly positive correlations with metabolites, while Phascolarctobacterium displayed predominantly negative correlations with metabolites. Granulicatella, on the other hand, was associated with a smaller number of metabolites, both positively and negatively. To delve deeper into the relationship between the metabolites linked to osteophyte formation and the genera, Spearman's correlation analysis was performed between the 3 genera and the 5 metabolites. The results demonstrated that Blautia was positively correlated with all 5 metabolites, whereas Phascolarctobacterium exhibited negative correlations with all of them (Figure 5B).
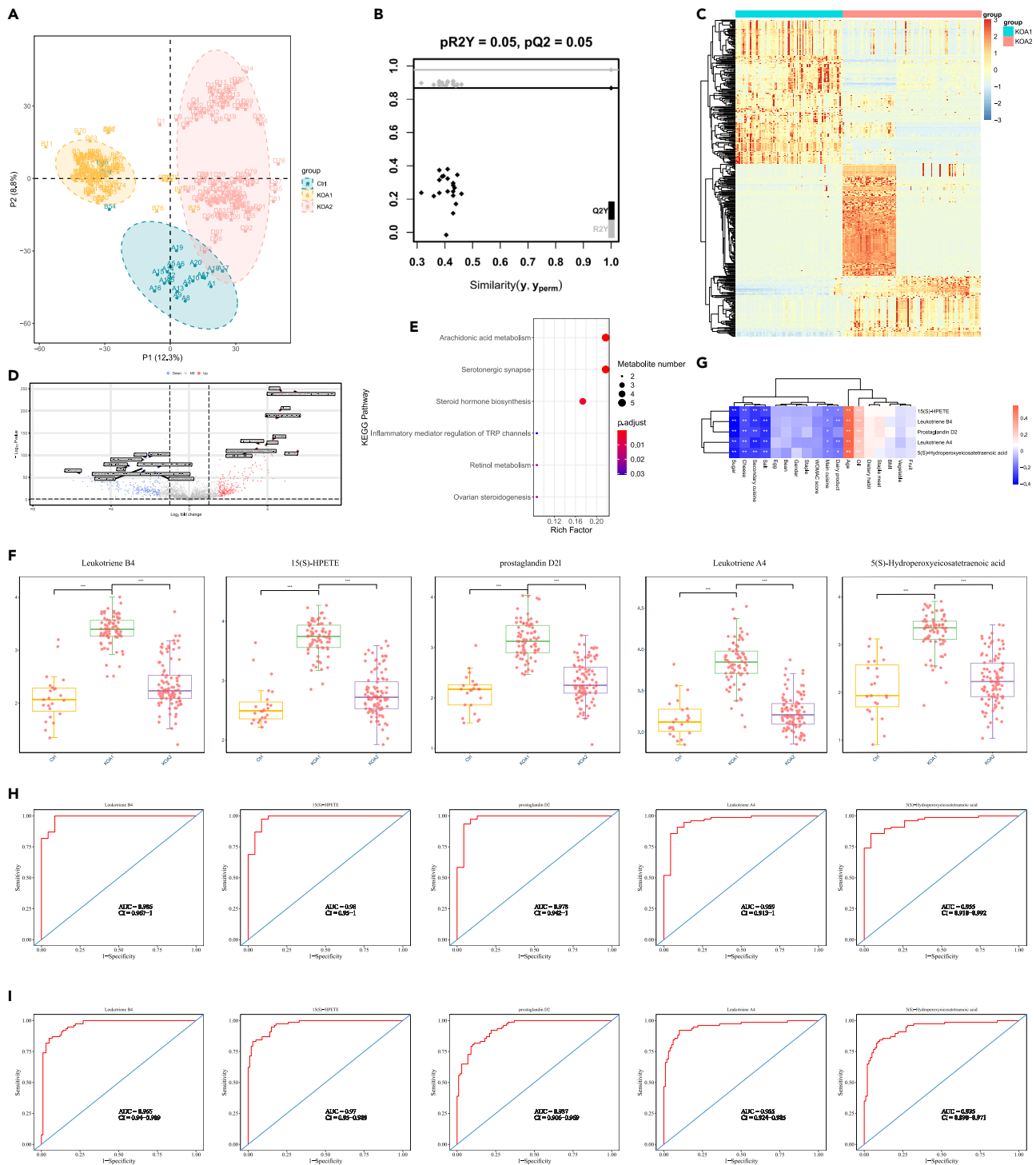
Figure 4. Alterations in serum metabolites associated with osteophyte formation in KOA

(A) PLS-DA scores showing the difference between the first two principal components (PCs) in the Ctrl, KOA1 and KOA2 groups.

(B) Validation of the model by 200 permutation test.

(C) Heatmap of differentially abundant metabolites based on relative abundance between KOA1 and KOA2 groups.

(D) Volcano plot showing the differential changes in metabolites between KOA1 and KOA2 groups.

Figure 4. Continued

(E) KEGG pathway enrichment scatterplot showing altered intestinal metabolic processes associated with osteophyte formation.

(F) Boxplot illustrating the 5 differentially enriched metabolites involved in the major altered pathway.

(G) Heatmap of the correlation between the 5 differentially enriched metabolites and clinical characteristics. ROC curves of the 5 differentially enriched metabolites in the (H) test cohort and (I) validation cohort. Positive correlations in red; negative correlations in blue. p-value, $*p < 0.05$; $**p < 0.01$; $***p < 0.001$. See also Figure S3 and Tables S6, S7, S8, S9, and S10.

DISCUSSION

OA predominantly affects the knee[16] and is characterized by joint space narrowing, osteophyte formation, and articular cartilage lesions.[17] The intestinal tract plays a pivotal role in human health, largely due to its prolonged interaction with gut microbiota. Some studies have suggested that gut microbiota contributes to the development of diseases.[18–20] Additionally, gut microbiota significantly influences serum metabolite levels.[21–23] Although the association between gut microbiota, serum metabolites, and OA has been increasingly recognized,[24–27] the specific correlation with osteophyte formation in KOA remains understudied. In this investigation, patients with KOA in Guangdong exhibited more prominent osteophyte formation and noticeable joint deformity in X-ray imaging, whereas patients in Inner Mongolia presented with fewer osteophytes but reported significant pain. This study aims to explore the correlation between gut microbiota, serum metabolites, and osteophyte formation in KOA.

A decrease in gut microbiota diversity is often considered indicative of chronic disease.[28,29] However, in our study, we observed an increase in alpha diversity in both the osteophyte and less osteophyte groups. Beta diversity revealed a shift in the composition of gut microbiota between the no osteophyte group and the osteophyte group, as well as between the less osteophyte group and the osteophyte group. Notably, Actinobacteria, Actinobacteriota, and Proteobacteria were more abundant in the osteophyte group, while Proteobacteria were diminished. Despite the commonly observed association of elevated F/B ratio with certain pathological conditions,[30,31] we did not find any difference in the F/B ratio between the osteophyte group and the no osteophyte group or less osteophyte group.

Certain genera such as Ruminococcaceae,[32] Roseburia,[33] and Faecalibacterium prausnitzii[34] in the gut are considered protective against OA, while others like Streptococcus, Fusobacterium,[32] Anaerotruncus, Oscillospira,[26] Desulfovibrio,[33] and Gemmiger[35] are considered harmful. Blautia, a genus within the Lachnospiraceae family in the Firmicutes phylum, has garnered attention for its role in metabolic diseases and antimicrobial activity against specific microorganisms.[36] In addition, Blautia is one of the most prevalent and important acid-producing bacteria in the gut, with high abundance and dominance among acid-producing strains of the family.[37,38] Blautia has potential probiotic properties[39] for the production of short-chain fatty acids (SCFAs),[40] which are beneficial for maintaining intestinal mucosal integrity and anti-inflammation.[41,42] Significant enrichment of Blautia species in the gut microbiota of OA patients.[43] In this study, we found that the abundance of Blautia in the feces of the test cohort osteophyte group was enriched compared to the test cohort no osteophyte group and the validation cohort less osteophyte group. In addition, Spearman's correlation analysis of the gut microbiota with clinical characteristics revealed that the abundance of Blautia in the feces was negatively correlated with meat eating habits, consumption of cheese and consumption of beans. This aligns with the local dietary habits in Inner Mongolia, where the population has a preference for cheese and meat, resulting in a reduced abundance of Blautia in the gut. The hypothesis that the lower osteophyte formation in KOA patients in Inner Mongolia is linked to reduced Blautia abundance due to dietary habits was further supported by LEfse analysis. Granulicatella, found in the normal flora of various body regions,[44,45] can become an opportunistic pathogen associated with invasive infections.[46,47] Phascolarctobacterium, a bacterium producing SCFAs,[48] is considered a representative probiotic.[49] The roles of Granulicatella and Phascolarctobacterium in OA are currently unexplored.

Furthermore, we observed that key serum metabolites in the osteophyte group were enriched in the arachidonic acid metabolic pathway, including Leukotriene B4, 15(S)-HPETE, prostaglandin D2, Leukotriene A4, and 5(S)-Hydroperoxyeicosatetraenoic acid. All these metabolites exhibited higher expression levels in the osteophyte group. Prostaglandin D2 (PGD2) is a crucial endogenous lipid mediator involved in arachidonic acid production, exerting its functions through g-protein-coupled receptors like the D prostaglandin receptor (DP1)[50] and chemotactic receptor homologs (CRTH2 or DP2).[51] PGD2 plays roles in physiological and pathological processes such as chemotaxis,[51] cellular transport,[52] bone metabolism,[53] and cancer.[54] Elevated levels of PGD2 have been reported in OA synovial fluid,[55] and it can influence nociception,[56,57] potentially contributing to the reduced pain observed in the osteophyte group compared to the less osteophyte group. Leukotriene B4 (LTB4) is produced from leukotriene A4 via leukotriene A4 hydrolase (LTA4H) in response to inflammatory stimuli.[58] Leukotriene A4 is a pro-inflammatory lipid mediator produced by membrane phospholipids through the enzymatic action of 5-lipoxygenase (5-LOX) on arachidonic acid (AA) during the initial stages of inflammation. LTB4, produced from leukotriene A4, has been associated with inflammatory arthritis and metabolic disorders.[59,60] It has been shown that patients with OA have elevated levels of LTB4 in synovium, synovial fluid, articular cartilage and subchondral bone.[61,62] Human OA subchondral osteoblasts constitutively produce LTB4.[61] Therefore, LTB4 in the serum of the osteophyte group may serve as a predictive marker for osteophyte formation in KOA, supported by ROC analysis showing an AUC value greater than 0.9 in both the test and validation cohorts. 5(S)- Hydroperoxyeicosatetraenoic acid (5(S)-HPETE), formed from arachidonic acid oxidation catalyzed by the enzyme 5-lipoxygenase,[63] remains unexplored in KOA. Spearman's correlation analysis of these 5 metabolites with clinical characteristics revealed that their expression levels were negatively correlated with dairy product consumption, beef consumption, cheese consumption, sugar and salt consumption, and positively correlated with age and oil consumption. This aligns with the results of the correlation analysis between gut microbiota and clinical characteristics.

In this study, we identified 3 genera associated with osteophyte formation in KOA, and their correlation with 42 metabolites was investigated. Notably, Blautia emerged as the central genus, and both Blautia[40] and Phascolarctobacterium[48] are known for their production of
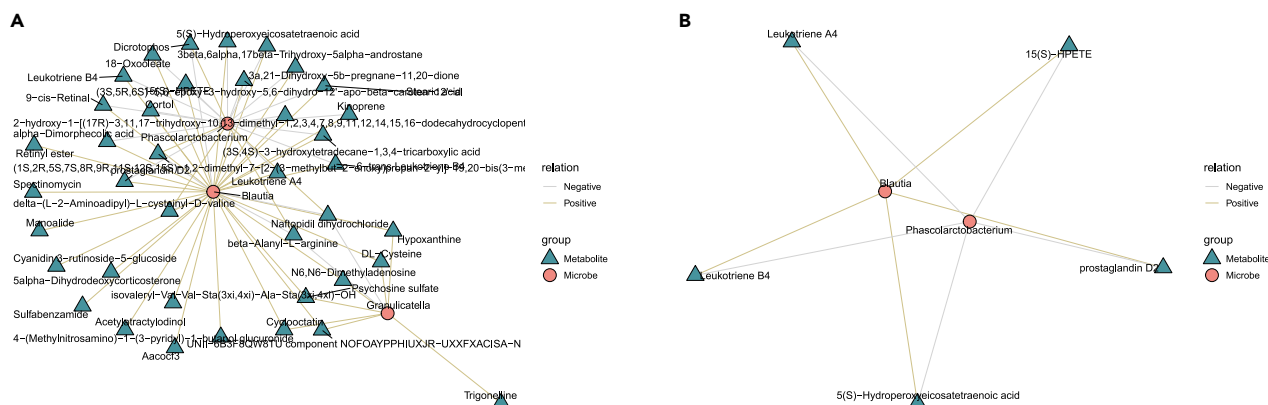
Figure 5. Correlation networks for osteophyte formation based on fecal microbiome and serum metabolome

Co-occurrence network plots showing the correlation between gut microbiota and serum metabolites (A) correlation with osteophyte formation in KOA and (B) involved in the major alteration pathways (Spearman's correlation analysis, r > 0.2, *p* < 0.05). Microorganisms are marked with circles and metabolites with triangles. Red connecting lines indicate positive correlations between nodes, while gray connecting lines indicate negative correlations. See also Table S11.

SCFAs. Although Blautia is enriched in the gut of OA patients,[43] its specific role in OA remains unknown. Phascolarctobacterium, on the other hand, has not been extensively studied in OA. Our analysis revealed a positive correlation between the 5 serum metabolites in the arachidonic acid pathway, screened by Blautia, and a negative correlation with Phascolarctobacterium. Among these 5 serum metabolites, LTB4 may serve as a predictive marker for osteophyte formation, while PGD2 could potentially alleviate pain in patients in the osteophyte group. Furthermore, we observed a negative correlation between fecal abundance of Blautia and the 5 metabolites, along with reduced cheese consumption. Therefore, we hypothesized that patients with KOA in Inner Mongolia have reduced osteophyte formation due to lower abundance of Blautia in the gut resulting from a local preference for cheese, which in turn causes lower levels of the 5 serum metabolites associated with the arachidonic acid pathway.

In conclusion, the findings indicated an enrichment of Blautia abundance in the KOA osteophyte group. Additionally, serum metabolites LTB4 and PGD2 were found to be expressed at higher levels in the KOA osteophyte group. Both the fecal abundance of Blautia and the levels of the 5 associated metabolites were negatively correlated with cheese consumption. Therefore, we hypothesize that elevated levels of Blautia in the gut may contribute to osteophyte formation in KOA patients, and serum metabolites LTB4 and PGD2 could potentially serve as biomarkers associated with osteophyte formation in KOA patients. Patients with KOA in Inner Mongolia might exhibit lower gut abundance of Blautia and decreased expression levels of the 5 associated serum metabolites due to the local preference for cheese, potentially leading to reduced osteophyte formation. While our results offer insights into changes in gut microbiota and serum metabolites resulting from diverse dietary habits in different regions associated with osteophyte formation in KOA patients, these observations should be further explored and confirmed through functional studies.

Limitations of the study

However, our study has some limitations. First, some patients with KOA in Guangdong experienced a better prognosis and did not return for follow-up, posing challenges in collecting comprehensive follow-up data. This resulted in incomplete clinical data for certain cases. Second, the identification of serum metabolites was conducted using untargeted LC-MS, and specific changes in metabolites could not be verified due to technical limitations. Lastly, our sample size was relatively small with limited cohort collection, and the findings require further validation in a large-scale multicenter study to strengthen the robustness of the conclusions.

STAR★METHODS

Detailed methods are provided in the online version of this paper and include the following:

- KEY RESOURCES TABLE
- RESOURCE AVAILABILITY
  - Lead contact
  - Materials availability
  - Data and code availability
- EXPERIMENTAL MODEL AND STUDY PARTICIPANT DETAILS
  - Recruitment of study participants
- METHOD DETAILS
  - Data/sample collection

○ Fecal DNA extraction, 16S rDNA gene sequencing and analysis
○ Untargeted metabolomics study
● QUANTIFICATION AND STATISTICAL ANALYSIS
○ Statistical analysis

SUPPLEMENTAL INFORMATION

Supplemental information can be found online at https://doi.org/10.1016/j.isci.2024.110111.

AUTHOR CONTRIBUTIONS

H.F., D.G., and X.Z.: Study conception and design; X.W.: Sample processing and data curation; D.Z., Z.X., and K.C.: Data analysis; D.Z., Z.X., K.C., X.W., and Y.F.: Data interpretation; D.Z.: Manuscript writing; D.G., H.F., and X.Z.: Manuscript editing and review; Y.F., C.Z., Z.P., and X.M.: Imaging acquisition; C.Z., Z.P., and X.M.: Supplementing sample additional data; H.F. and D.G.: Study supervision and funding acquisition. All authors reviewed the results and approved the final version of the manuscript.

DECLARATION OF INTERESTS

The authors declare no competing interests.

REFERENCES

1. Palazzo, C., Nguyen, C., Lefevre-Colau, M.-M., Rannou, F., and Poiraudeau, S. (2016). Risk factors and burden of osteoarthritis. Ann. Phys. Rehabil. Med. *59*, 134–138. https://doi.org/10.1016/j.rehab.2016.01.006.

2. Losina, E., Weinstein, A.M., Reichmann, W.M., Burbine, S.A., Solomon, D.H., Daigle, M.E., Rome, B.N., Chen, S.P., Hunter, D.J., Suter, L.G., et al. (2013). Lifetime risk and age at diagnosis of symptomatic knee osteoarthritis in the US. Arthritis Care Res. *65*, 703–711. https://doi.org/10.1002/acr.21898.

3. Li, D., Li, S., Chen, Q., and Xie, X. (2020). The Prevalence of Symptomatic Knee Osteoarthritis in Relation to Age, Sex, Area, Region, and Body Mass Index in China: A Systematic Review and Meta-Analysis. Front. Med. *7*, 304. https://doi.org/10.3389/fmed.2020.00304.

4. Vina, E.R., and Kwoh, C.K. (2018). Epidemiology of osteoarthritis: literature update. Curr. Opin. Rheumatol. *30*, 160–167. https://doi.org/10.1097/BOR.0000000000000479.

5. Jin, X., Beguerie, J.R., Zhang, W., Blizzard, L., Otahal, P., Jones, G., and Ding, C. (2015). Circulating C reactive protein in osteoarthritis: a systematic review and meta-analysis. Ann. Rheum. Dis. *74*, 703–710. https://doi.org/10.1136/annrheumdis-2013-204494.

6. Iqbal, J., Yuen, T., Sun, L., and Zaidi, M. (2016). From the gut to the strut: where inflammation reigns, bone abstains. J. Clin. Invest. *126*, 2045–2048. https://doi.org/10.1172/JCI87430.

7. Yu, X.H., Yang, Y.Q., Cao, R.R., Bo, L., and Lei, S.F. (2021). The causal role of gut microbiota in development of osteoarthritis. Osteoarthritis Cartilage *29*, 1741–1750. https://doi.org/10.1016/j.joca.2021.08.003.

8. Liu, L., Tian, F., Li, G.-Y., Xu, W., and Xia, R. (2022). The effects and significance of gut microbiota and its metabolites on the regulation of osteoarthritis: Close coordination of gut-bone axis. Front. Nutr. *9*, 1012087. https://doi.org/10.3389/fnut.2022.1012087.

9. Sandell, L.J., and Aigner, T. (2001). Articular cartilage and changes in arthritis. An introduction: cell biology of osteoarthritis. Arthritis Res. *3*, 107–113.

10. Matyas, J.R., Sandell, L.J., and Adams, M.E. (1997). Gene expression of type II collagens in chondro-osteophytes in experimental osteoarthritis. Osteoarthritis Cartilage *5*, 99–105.

11. van der Kraan, P.M., and van den Berg, W.B. (2007). Osteophytes: relevance and biology. Osteoarthritis Cartilage *15*, 237–244.

12. Ulici, V., Kelley, K.L., Azcarate-Peril, M.A., Cleveland, R.J., Sartor, R.B., Schwartz, T.A., and Loeser, R.F. (2018). Osteoarthritis induced by destabilization of the medial meniscus is reduced in germ-free mice. Osteoarthritis Cartilage *26*, 1098–1109. https://doi.org/10.1016/j.joca.2018.05.016.

13. Altman, R., Asch, E., Bloch, D., Bole, G., Borenstein, D., Brandt, K., Christy, W., Cooke, T.D., Greenwald, R., and Hochberg, M. (1986). Development of criteria for the classification and reporting of osteoarthritis. Classification of osteoarthritis of the knee. Diagnostic and Therapeutic Criteria Committee of the American Rheumatism Association. Arthritis Rheum. *29*, 1039–1049.

14. Wu, K.-T., Wang, Y.-W., Wu, R.-W., Huang, C.C., and Chen, Y.-C. (2023). Association of a femoral neck T score with knee joint osteophyte formation but not with skeletal muscle mass. Clin. Rheumatol. *42*, 917–922. https://doi.org/10.1007/s10067-022-06410-w.

15. Wikoff, W.R., Anfora, A.T., Liu, J., Schultz, P.G., Lesley, S.A., Peters, E.C., and Siuzdak, G. (2009). Metabolomics analysis reveals large effects of gut microflora on mammalian blood metabolites. Proc. Natl. Acad. Sci. USA *106*, 3698–3703. https://doi.org/10.1073/pnas.0812874106.

16. Barnett, R. (2018). Osteoarthritis. Lancet *391*, 1985. https://doi.org/10.1016/S0140-6736(18)31064-X.

17. van den Bosch, M.H.J. (2021). Osteoarthritis year in review 2020: biology. Osteoarthritis Cartilage *29*, 143–150. https://doi.org/10.1016/j.joca.2020.10.006.

18. Hu, X., Guo, J., Zhao, C., Jiang, P., Maimai, T., Yanyi, L., Cao, Y., Fu, Y., and Zhang, N. (2020). The gut microbiota contributes to the development of Staphylococcus aureus-induced mastitis in mice. ISME J. *14*, 1897–1910. https://doi.org/10.1038/s41396-020-0651-1.

19. Hu, X., He, Z., Zhao, C., He, Y., Qiu, M., Xiang, K., Zhang, N., and Fu, Y. (2024). Gut/rumen-mammary gland axis in mastitis: Gut/rumen microbiota-mediated "gastroenterogenic

mastitis". J. Adv. Res. 55, 159–171. https://doi.org/10.1016/j.jare.2023.02.009.

20. He, Z., Zhao, C., He, Y., Liu, Z., Fan, G., Zhu, K., Wang, Y., Zhang, N., Fu, Y., and Hu, X. (2023). Enterogenic Stenotrophomonas maltophilia migrates to the mammary gland to induce mastitis by activating the calcium-ROS-AMPK-mTOR-autophagy pathway. J. Anim. Sci. Biotechnol. 14, 157. https://doi.org/10.1186/s40104-023-00952-y.

21. Marcobal, A., Kashyap, P.C., Nelson, T.A., Aronov, P.A., Donia, M.S., Spormann, A., Fischbach, M.A., and Sonnenburg, J.L. (2013). A metabolomic view of how the human gut microbiota impacts the host metabolome using humanized and gnotobiotic mice. ISME J. 7, 1933–1943. https://doi.org/10.1038/ismej.2013.89.

22. Wilmanski, T., Rappaport, N., Earls, J.C., Magis, A.T., Manor, O., Lovejoy, J., Omenn, G.S., Hood, L., Gibbons, S.M., and Price, N.D. (2019). Blood metabolome predicts gut microbiome α-diversity in humans. Nat. Biotechnol. 37, 1217–1228. https://doi.org/10.1038/s41587-019-0233-9.

23. Lee-Sarwar, K.A., Lasky-Su, J., Kelly, R.S., Litonjua, A.A., and Weiss, S.T. (2020). Metabolome-Microbiome Crosstalk and Human Disease. Metabolites 10, 181. https://doi.org/10.3390/metabo10050181.

24. Lan, H., Hong, W., Qian, D., Peng, F., Li, H., Liang, C., Du, M., Gu, J., Mai, J., Bai, B., and Peng, G. (2021). Quercetin modulates the gut microbiota as well as the metabolome in a rat model of osteoarthritis. Bioengineered 12, 6240–6250. https://doi.org/10.1080/21655979.2021.1969194.

25. Collins, K.H., Paul, H.A., Reimer, R.A., Seerattan, R.A., Hart, D.A., and Herzog, W. (2015). Relationship between inflammation, the gut microbiota, and metabolic osteoarthritis development: studies in a rat model. Osteoarthritis Cartilage 23, 1989–1998. https://doi.org/10.1016/j.joca.2015.03.014.

26. Loeser, R.F., Arbeeva, L., Kelley, K., Fodor, A.A., Sun, S., Ulici, V., Longobardi, L., Cui, Y., Stewart, D.A., Sumner, S.J., et al. (2022). Association of Increased Serum Lipopolysaccharide, But Not Microbial Dysbiosis, With Obesity-Related Osteoarthritis. Arthritis Rheumatol. 74, 227–236. https://doi.org/10.1002/art.41955.

27. Li, K., Liu, A., Zong, W., Dai, L., Liu, Y., Luo, R., Ge, S., and Dong, G. (2021). Moderate exercise ameliorates osteoarthritis by reducing lipopolysaccharides from gut microbiota in mice. Saudi J. Biol. Sci. 28, 40–49. https://doi.org/10.1016/j.sjbs.2020.08.027.

28. Eckburg, P.B., Bik, E.M., Bernstein, C.N., Purdom, E., Dethlefsen, L., Sargent, M., Gill, S.R., Nelson, K.E., and Relman, D.A. (2005). Diversity of the human intestinal microbial flora. Science 308, 1635–1638.

29. Pascal, V., Pozuelo, M., Borruel, N., Casellas, F., Campos, D., Santiago, A., Martinez, X., Varela, E., Sarrabayrouse, G., Machiels, K., et al. (2017). A microbial signature for Crohn's disease. Gut 66, 813–822. https://doi.org/10.1136/gutjnl-2016-313235.

30. Masumoto, S., Terao, A., Yamamoto, Y., Mukai, T., Miura, T., and Shoji, T. (2016). Non-absorbable apple procyanidins prevent obesity associated with gut microbial and metabolic changes. Sci. Rep. 6, 31208. https://doi.org/10.1038/srep31208.

31. Khan, R., Sharma, A., Ravikumar, R., Parekh, A., Srinivasan, R., George, R.J., and Raman, R.

(2021). Association Between Gut Microbial Abundance and Sight-Threatening Diabetic Retinopathy. Invest. Ophthalmol. Vis. Sci. 62, 19. https://doi.org/10.1167/iovs.62.7.19.

32. Huang, J., Chen, J., Li, B., Zeng, B., Chou, C.-H., Zheng, X., Xie, J., Li, H., Hao, Y., Chen, G., et al. (2020). Faecal microbiota transplantation from metabolically compromised human donors accelerates osteoarthritis in mice. Ann. Rheum. Dis. 79, 646–656. https://doi.org/10.1136/annrheumdis-2019-216471.

33. Wei, J., Zhang, C., Zhang, Y., Zhang, W., Doherty, M., Yang, T., Zhai, G., Obotiba, A.D., Lyu, H., Zeng, C., and Lei, G. (2021). Association Between Gut Microbiota and Symptomatic Hand Osteoarthritis: Data From the Xiangya Osteoarthritis Study. Arthritis Rheumatol. 73, 1656–1662. https://doi.org/10.1002/art.41729.

34. Chen, J., Wang, A., and Wang, Q. (2021). Dysbiosis of the gut microbiome is a risk factor for osteoarthritis in older female adults: a case control study. BMC Bioinformatics 22, 299. https://doi.org/10.1186/s12859-021-04199-0.

35. Wang, Z., Zhu, H., Jiang, Q., and Zhu, Y.Z. (2021). The gut microbiome as non-invasive biomarkers for identifying overweight people at risk for osteoarthritis. Microb. Pathog. 157, 104976. https://doi.org/10.1016/j.micpath.2021.104976.

36. Kalyana Chakravarthy, S., Jayasudha, R., Sai Prashanthi, G., Ali, M.H., Sharma, S., Tyagi, M., and Shivaji, S. (2018). Dysbiosis in the Gut Bacterial Microbiome of Patients with Uveitis, an Inflammatory Disease of the Eye. Indian J. Microbiol. 58, 457–469. https://doi.org/10.1007/s12088-018-0746-9.

37. Zhang, W., Li, J., Lu, S., Han, N., Miao, J., Zhang, T., Qiang, Y., Kong, Y., Wang, H., Gao, T., et al. (2019). Gut microbiota community characteristics and disease-related microorganism pattern in a population of healthy Chinese people. Sci. Rep. 9, 1594. https://doi.org/10.1038/s41598-018-36318-y.

38. Vacca, M., Celano, G., Calabrese, F.M., Portincasa, P., Gobbetti, M., and De Angelis, M. (2020). The Controversial Role of Human Gut Lachnospiraceae. Microorganisms 8, 573. https://doi.org/10.3390/microorganisms8040573.

39. Liu, X., Mao, B., Gu, J., Wu, J., Cui, S., Wang, G., Zhao, J., Zhang, H., and Chen, W. (2021). Blautia-a new functional genus with potential probiotic properties? Gut Microbes 13, 1–21. https://doi.org/10.1080/19490976.2021.1875796.

40. Yang, Y.-N., Wang, Q.-C., Xu, W., Yu, J., Zhang, H., and Wu, C. (2022). The berberine-enriched gut commensal Blautia producta ameliorates high-fat diet (HFD)-induced hyperlipidemia and stimulates liver LDLR expression. Biomed Pharmacother 155, 113749. https://doi.org/10.1016/j.biopha.2022.113749.

41. Davila, A.-M., Blachier, F., Gotteland, M., Andriamihaja, M., Benetti, P.-H., Sanz, Y., and Tomé, D. (2013). Intestinal luminal nitrogen metabolism: role of the gut microbiota and consequences for the host. Pharmacol. Res. 68, 95–107. https://doi.org/10.1016/j.phrs.2012.11.005.

42. Morrison, D.J., and Preston, T. (2016). Formation of short chain fatty acids by the gut microbiota and their impact on human metabolism. Gut Microbes 7, 189–200. https://doi.org/10.1080/19490976.2015.1134082.

43. Chen, C., Zhang, Y., Yao, X., Li, S., Wang, G., Huang, Y., Yang, Y., Zhang, A., Liu, C., Zhu, D., et al. (2023). Characterizations of the Gut Bacteriome, Mycobiome, and Virome in Patients with Osteoarthritis. Microbiol. Spectr. 11, e0171122. https://doi.org/10.1128/spectrum.01711-22.

44. Ruoff, K.L. (1991). Nutritionally variant streptococci. Clin. Microbiol. Rev. 4, 184–190.

45. Mikkelsen, L., Theilade, E., and Poulsen, K. (2000). Abiotrophia species in early dental plaque. Oral Microbiol. Immunol. 15, 263–268.

46. Li, M., Li, K., Tang, S., Lv, Y., Wang, Q., Wang, Z., Luo, B., Niu, J., Zhu, Y., Guo, W., et al. (2022). Restoration of the gut microbiota is associated with a decreased risk of hepatic encephalopathy after TIPS. JHEP Rep. 4, 100448. https://doi.org/10.1016/j.jhepr.2022.100448.

47. Elfessi, Z., Liu, E., Dukarevich, Y., Caniff, K., Marquez, K., and Shabbir, Z. (2019). Sepsis induced bacterial peritonitis caused by Granulicatella adiacens. Am. J. Emerg. Med. 37, 2263.e1–2263.e3. https://doi.org/10.1016/j.ajem.2019.158428.

48. Wu, F., Guo, X., Zhang, J., Zhang, M., Ou, Z., and Peng, Y. (2017). Phascolarctobacterium faecium abundant colonization in human gastrointestinal tract. Exp. Ther. Med. 14, 3122–3126. https://doi.org/10.3892/etm.2017.4878.

49. Sherman, S.B., Sarsour, N., Salehi, M., Schroering, A., Mell, B., Joe, B., and Hill, J.W. (2018). Prenatal androgen exposure causes hypertension and gut microbiota dysbiosis. Gut Microbes 9, 400–421. https://doi.org/10.1080/19490976.2018.1441664.

50. Hirata, M., Kakizuka, A., Aizawa, M., Ushikubi, F., and Narumiya, S. (1994). Molecular characterization of a mouse prostaglandin D receptor and functional expression of the cloned gene. Proc. Natl. Acad. Sci. USA 91, 11192–11196.

51. Hirai, H., Tanaka, K., Yoshie, O., Ogawa, K., Kenmotsu, K., Takamori, Y., Ichimasa, M., Sugamura, K., Nakamura, M., Takano, S., and Nagata, K. (2001). Prostaglandin D2 selectively induces chemotaxis in T helper type 2 cells, eosinophils, and basophils via seven-transmembrane receptor CRTH2. J. Exp. Med. 193, 255–261.

52. Ahmed, S.R., McGettrick, H.M., Yates, C.M., Buckley, C.D., Ratcliffe, M.J., Nash, G.B., and Rainger, G.E. (2011). Prostaglandin D2 regulates CD4+ memory T cell trafficking across blood vascular endothelium and primes these cells for clearance across lymphatic endothelium. J. Immunol. 187, 1432–1439. https://doi.org/10.4049/jimmunol.1100299.

53. Yue, L., Haroun, S., Parent, J.-L., and de Brum-Fernandes, A.J. (2014). Prostaglandin D(2) induces apoptosis of human osteoclasts through ERK1/2 and Akt signaling pathways. Bone 60, 112–121. https://doi.org/10.1016/j.bone.2013.12.011.

54. Omori, K., Morikawa, T., Kunita, A., Nakamura, T., Aritake, K., Urade, Y., Fukayama, M., and Murata, T. (2018). Lipocalin-type prostaglandin D synthase-derived PGD2 attenuates malignant properties of tumor endothelial cells. J. Pathol. 244, 84–96. https://doi.org/10.1002/path.4993.

55. Zayed, N., Li, X., Chabane, N., Benderdour, M., Martel-Pelletier, J., Pelletier, J.-P., Duval, N., and Fahmi, H. (2008). Increased expression of lipocalin-type prostaglandin D2

synthase in osteoarthritic cartilage. Arthritis Res. Ther. *10*, R146. https://doi.org/10.1186/ar2581.

56. Eguchi, N., Minami, T., Shirafuji, N., Kanaoka, Y., Tanaka, T., Nagata, A., Yoshida, N., Urade, Y., Ito, S., and Hayaishi, O. (1999). Lack of tactile pain (allodynia) in lipocalin-type prostaglandin D synthase-deficient mice. Proc. Natl. Acad. Sci. USA *96*, 726–730.

57. Minami, T., Okuda-Ashitaka, E., Nishizawa, M., Mori, H., and Ito, S. (1997). Inhibition of nociceptin-induced allodynia in conscious mice by prostaglandin D2. Br. J. Pharmacol. *122*, 605–610.

58. Henderson, W.R. (1994). The role of leukotrienes in inflammation. Ann. Intern. Med. *121*, 684–697.

59. Shao, W.-H., Del Prete, A., Bock, C.B., and Haribabu, B. (2006). Targeted disruption of leukotriene B4 receptors BLT1 and BLT2: a critical role for BLT1 in collagen-induced arthritis in mice. J. Immunol. *176*, 6254–6261.

60. Spite, M., Hellmann, J., Tang, Y., Mathis, S.P., Kosuri, M., Bhatnagar, A., Jala, V.R., and Haribabu, B. (2011). Deficiency of the leukotriene B4 receptor, BLT-1, protects against systemic insulin resistance in diet-induced obesity. J. Immunol. *187*, 1942–1949. https://doi.org/10.4049/jimmunol.1100196.

61. Paredes, Y., Massicotte, F., Pelletier, J.-P., Martel-Pelletier, J., Laufer, S., and Lajeunesse, D. (2002). Study of the role of leukotriene B4 in abnormal function of human subchondral osteoarthritis osteoblasts:

effects of cyclooxygenase and/or 5-lipoxygenase inhibition. Arthritis Rheum. *46*, 1804–1812.

62. Hashimoto, A., Endo, H., Hayashi, I., Murakami, Y., Kitasato, H., Kono, S., Matsui, T., Tanaka, S., Nishimura, A., Urabe, K., et al. (2003). Differential expression of leukotriene B4 receptor subtypes (BLT1 and BLT2) in human synovial tissues and synovial fluid leukocytes of patients with rheumatoid arthritis. J. Rheumatol. *30*, 1712–1718.

63. Samuelsson, B. (1983). Leukotrienes: mediators of immediate hypersensitivity reactions and inflammation. Science *220*, 568–575.

STAR★METHODS

KEY RESOURCES TABLE

REAGENT or RESOURCE	SOURCE	IDENTIFIER
Biological samples		
Fecal samples	This paper	NCBI Sequence Read Archive (SRA): PRJNA1111278 (http://www.ncbi.nlm.nih.gov/bioproject/1111278)
Serum samples	This paper	MetaboLights (https://www.ebi.ac.uk/metabolights/MTBLS10192)
Critical commercial assays		
Phusion® High-Fidelity PCR Master Mix	New England Biolabs, USA	Cat#M0532S
MinElute PCR Purification Kit	Qiagen, Germany	Cat#28004
TruSeq® DNA PCR-Free Sample Preparation Kit	Illumina, USA	Cat#E7370L
Deposited data		
RNA-seq data	This paper	NCBI Sequence Read Archive (SRA): PRJNA1111278 (http://www.ncbi.nlm.nih.gov/bioproject/1111278)
Untargeted metabolomics data	This paper	MetaboLights (https://www.ebi.ac.uk/metabolights/MTBLS10192)
Oligonucleotides		
Specific primers with barcodes (314F: CCTAYGGGRBGCASCAG, 806R: CCTAYGGGRBGCASCAG)	This paper	N/A
Software and algorithms		
R version 4.3.2	CRAN	https://cran.r-project.org/bin/windows/base/old/4.3.2/
UPARSE v7.0.1001	N/A	http://www.drive5.com/uparse/
Analyst TF 1.7.1 software	Sciex, Concord, ON, Canada	https://sciex.com/br/products/software/analyst-tf-software

RESOURCE AVAILABILITY

Lead contact

Further information and requests for resources and reagents should be directed to and will be fulfilled by the lead contact, Huolun Feng (fenghuolun2022@qq.com).

Materials availability

This study did not generate new unique reagents.

Data and code availability

- Raw 16S rDNA gene sequencing data generated by next-generation sequencing platforms, with per-base quality scores, have been deposited at NCBI Sequence Read Archive (SRA) at http://www.ncbi.nlm.nih.gov/bioproject/1111278, and are publicly available as of the date of publication. Accession numbers are listed in the key resources table.
- Metabolomics data have been deposited at MetaboLights (https://www.ebi.ac.uk/metabolights/MTBLS10192) and are publicly available as of the date of publication. Accession numbers are listed in the key resources table.
- This paper does not report the original code.
- Any additional information required to re-analyze the data reported in this paper is available from the lead contact upon request.

EXPERIMENTAL MODEL AND STUDY PARTICIPANT DETAILS

Recruitment of study participants

For this investigation, we recruited a total of 20 healthy volunteers and 80 KOA patients from Guangdong Provincial Hospital of Chinese Medicine in the Guangdong region. The recruitment period spanned from July 2022 to July 2023. Additionally, 100 KOA patients were enrolled from Ewenke Banner People's Hospital in the Inner Mongolia region. The diagnosis of KOA in all patients adhered to the criteria established by the American College of Rheumatology. Inclusion Criteria: (i) Normal results in rheumatoid, autoimmune, or infection index tests. (ii) Absence of previous knee trauma or surgery, and no extra-articular deformities. (iii) Normal results in fecal parasite tests, with no history of abnormal bowel movements or gastrointestinal disease episodes. (iv) No prolonged use of antibiotics in the medical history. Exclusion Criteria: (i) Long-term requirement for immunosuppressants or antibiotics exceeding one year. (ii) Chronic enteritis with recurrent diarrhea in the last month. (iii) Patients with intestinal cancer or those who have undergone intestinal surgery.

The mean age of the patients in this study was 64 ± 7.9 years, with a BMI of 26 ± 3.6 kg/m^2. Of the participants, 80.5% were female, and gender did not influence the results. All participants provided informed consent, and the research protocol received approval from the Institutional Review Board of the Ethics Committee of Guangdong Provincial Hospital of Chinese Medicine (BE2022-174-01).

METHOD DETAILS

Data/sample collection

Photographs of both knees in a standing position were captured for healthy volunteers and KOA patients from Guangdong Provincial Hospital of Chinese Medicine and KOA patients from Ewenke Banner People's Hospital using flat films. Participants were stratified into 3 groups based on the K-L grading system: (i) Ctrl group (no osteophyte group): Consisting of participants from Guangdong Provincial Hospital of Chinese Medicine with K-L grade 0–1; (ii) KOA1 group (osteophyte group): Comprising participants from Guangdong Provincial Hospital of Chinese Medicine with K-L grade 2–4; and (iii) KOA2 group (less osteophyte group): Comprising KOA patients from Ewenke Banner People's Hospital, serving as a validation cohort. Approximately 3 mL of venous blood was collected from all 3 groups by nurses. Following collection, the blood specimens underwent centrifugation at a speed of 4000 r/min for 10–30 min. Subsequently, the upper serum layer was carefully extracted into freezing tubes using a pipette gun. Fecal samples from all participants were collected in plastic containers on ice and promptly transported to the laboratory within 2 h. Upon arrival, the fecal samples were transferred to 2 mL eppendorf tubes. After the collection process, both serum and fecal specimens were stored in a $-80°C$ refrigerator for further analysis.

Fecal DNA extraction, 16S rDNA gene sequencing and analysis

DNA extraction from fecal samples was conducted using the cetyltrimethylammonium bromide or sodium dodecyl sulfate (CTAB/SDS) method. Initially, DNA concentration and purity were assessed on agarose gels, followed by dilution of the DNA to 1 ng/μL with sterile water. Specific primers with barcodes (314F: CCTAYGGGRBGCASCAG and 806R: CCTAYGGGRBGCASCAG) and Phusion High-Fidelity PCR Master Mix with GC Buffer (New England Biolabs, USA) were utilized to amplify the V3-V4 region of the 16S rRNA gene using a PCR system (BIO-RAD, USA). The resulting PCR product mixture was purified with a MinElute PCR Purification Kit (Qiagen, Germany). Sequencing libraries were generated using the TruSeq DNA PCR-Free Sample Preparation Kit (Illumina, USA) following the manufacturer's instructions. Library quality was assessed using a Qubit 2.0 Fluorometer (Thermo Fisher, USA) and Q-PCR. Subsequently, the library was sequenced on the NovaSeq6000 system (Illumina, USA). The UPARSE algorithm (UPARSEv7.0.1001, http://www.drive5.com/uparse/) was employed for sequence analysis, where sequences with ≥97% similarity were grouped into operational taxonomic units (OTUs). Abundance information of the OTUs was normalized based on the sequence number corresponding to the sample with the lowest number of sequences. Additionally, alpha diversity analysis was conducted using the vegan package in R (Version 4.3.2). Beta diversity calculations were performed using principal coordinate analysis (PCoA) to assess diversity in samples for species complexity. Bacterial abundance and diversity were compared using the Wilcoxon rank-sum test. Linear discriminant analysis effect size (LEfSe) was used to analyze the relative abundance of bacterial populations.

Untargeted metabolomics study

Serum samples stored at $-80°C$ were thawed on ice and vortexed for 10 s. Subsequently, 50 μL of the sample containing the internal standard and 300 μL of extraction solution (ACN: methanol = 1:4, V/V) were added to a 2 mL microcentrifuge tube. The sample underwent vortexing for 3 min and then centrifugation at 12000 rpm for 10 min (4°C). From the supernatant, 200 μL was collected, placed at $-20°C$ for 30 min, and then centrifuged at 12000 rpm for 3 min at 4°C. For LC-MS analysis, 180 μL of the supernatant was utilized. All serum samples were processed using the LC-MS system according to the machine instructions. The analytical conditions were as follows: UPLC: chromatographic column Waters ACQUITY UPLC BEH C18 1.8 μm/2.1 mm * 100 mm; column temperature, 40°C; flow rate: 0.4 mL/min; injection volume, 2 μL; solvent system: water (0.1% formic acid): acetonitrile (0.1% formic acid); elution of the column with 5% mobile phase B (0.1% formic acid acetonitrile) at an elution time of 0 min, followed by a linear gradient elution to 90% mobile phase B (0.1% formic acid acetonitrile) with an elution time of 11 min, a hold time of 1 min, and then a return to 5% mobile phase B within 0.1 min, a hold time of 1.9 min, and then a rapid return to starting conditions. Data were collected in information dependent acquisition (IDA) mode using Analyst TF 1.7.1 software (Sciex, Concord, ON, Canada). Source parameters were set as follows: ion source gas1 (gas1), 50 psi; ion source gas2 (GAS2), 50 psi; curtain gas (CUR), 35 psi; temperature (TEM), 550°C, or 450°C; cluster scattering potential (DP), 60v, - 60v in positive and negative modes, respectively; and ion spray floatation pressure (ISVF), 5000v or -4000v in positive and negative modes, respectively. The TOF MS scan parameters were set as follows: mass range,

50–1000 Da; accumulation time, 200 ms; dynamic background subtraction, on. The product ion scan parameters were set as follows: mass range 25–1000 Da; accumulation time, 40 ms; collision energy, 30 or - 30 V in positive or negative mode, respectively; collision energy spread, 15; resolution, units; charge state, 1 to 1; intensity, 100 cps; isotopes up to 4 Da were excluded; mass tolerance, 50 mDa; and the maximum number of candidate ions to be monitored per cycle was 12. The raw data files acquired by LC-MS were converted to mzXML format by ProteoWizard software. Peak extraction, peak alignment, and retention time correction were performed using the XCMS program. The peak area was corrected by the "SVR" method. Peaks with less than a 50% detection rate were discarded in each set of samples. Metabolic identification information was obtained by searching the laboratory's own database, a comprehensive public database, the AI database, and metDNA.

QUANTIFICATION AND STATISTICAL ANALYSIS

Statistical analysis

Univariate and multivariate logistic regression analyses were conducted, with the presence or absence of osteophyte formation serving as the dependent variable and clinical characteristics as the independent variables. Following the normalization of ASV abundance, the Kruskal-Wallis test was utilized to assess the alpha and beta diversity of ASVs between groups. Differential expression was identified using Student's t test and fold change (FC) values. The Wilcoxon test was applied to compare the differential gut microbiota between the two groups. Spearman's correlation analysis was employed to calculate correlations between species and clinical information, metabolites and clinical information, as well as species and metabolites. Statistical significance was determined when $p < 0.05$. All data analyses were performed using R version 4.3.2 (R Foundation for Statistical Computing).